# Subcritical Magnetohydrodynamic Turbulence

R. E. Waltz
*GA Technologies Inc., San Diego, California 92138*
(Received 15 March 1985)

Numerical simulations of a simple model for ideal magnetohydrodynamic modes have shown stationary turbulence and transport at $\beta$ values substantially below the critical $\beta$ required for linear instability. The phenomena appears to be similar to subcritical turbulence in plane-parallel pipe flow.

PACS numbers: 52.30.Gz, 52.35.Ra

A system with self-sustained turbulent motion having a parameter below the critical value for the onset of linear instability is said to exhibit "subcritical turbulence." In this Letter I report on numerical simulations of a simple model for magnetohydrodynamic (MHD) ballooning modes which has homogeneous stationary-state turbulence with large transport at values of $\beta$ (ratio of plasma to magnetic pressure) substantially below the critical $\beta$ for linear stability. At low to moderate $\beta$, it is generally believed that short-wavelength dissipative modes of one kind or another are linearly unstable and are the prevailing cause of turbulent energy transport in tokamaks and other fusion devices. However, the onset of longer-wavelength MHD modes (usually called high-$n$ ballooning modes) at the critical $\beta$ is expected to result in such large mixing lengths and therefore large transport rates as to completely limit the $\beta$ and the energy content of the tokamak plasmas. Thus evidence for possible subcritical turbulence among these catastrophic ideal MHD modes is of great practical interest.

Subcritical turbulence is a well-known feature of several (but not all) types of hydrodynamic flows.[1] The best understood case is that of plane-parallel (Poiseuille) pipe flow.[2,3] Both experimentally and in numerical simulations, the flow becomes turbulent at values of the Reynolds number several times smaller than the critical value for linear instability. In what follows, I shall make some partial but hopefully useful analogies with the case of pipe flow. Established examples of subcritical turbulence from plasma physics are more recent and less well known.[4,5]

For the case at hand, the simple homogeneous two-dimensional MHD model assumes that each mode labeled by its wave number $\mathbf{k}_\perp$ across the magnetic field balloons to the bad-curvature region on the outside of the tokamak. Ignoring the potentially important role of shear in the magnetic field direction and the three-dimensional aspects of the ballooning modes, we assume that each mode has a fixed effective average parallel-field wave number $k_\parallel$ corresponding to an inverse connection length $Rq$ and an effective average curvature drift $g$ equal to $L_p/R$ times the diamagnetic drift. $L_p^{-1}$ is the inverse equilibrium pressure-gradient length which drives the modes, $R$ is the tokamak major radius, and $q$ is the safety factor. The model consists of a vorticity equation, an Ohm's law, and a pressure convection equation to advance the perturbations in the electric potential $\tilde{\phi}$, the parallel vector potential $\tilde{A}$, and the pressure $\tilde{P}$:

$$\frac{\tilde{d}}{dt}k_\perp^2\tilde{\phi}_k = ig\omega_*\tilde{P}_k - \tilde{\nabla}_\parallel(k_\perp^2\tilde{A}_k) - \gamma_k^\phi k_\perp^2\phi_k, \tag{1}$$

$$\frac{\partial}{\partial t}\tilde{A}_k = -\frac{\tilde{\nabla}_\parallel}{\beta}\tilde{\phi}_k - \gamma_k^A\tilde{A}_k, \tag{2}$$

$$\frac{\tilde{d}}{dt}\tilde{P}_k = -i\omega_*\tilde{\phi}_k - \gamma_k^P\tilde{P}_k. \tag{3}$$

The nonlinear mode couplings are contained in the $\tilde{\mathbf{E}}\times\mathbf{B}_0$ convective time derivative $(\partial/\partial t + \tilde{\mathbf{V}}_E\cdot\nabla_\perp)$ and the magnetic flutter of the parallel gradient $(\nabla_\parallel + \tilde{\mathbf{B}}_\perp/B_0\cdot\nabla_\perp)$,

$$\frac{\tilde{d}}{dt}\tilde{f}_k = \frac{\partial}{\partial t}\tilde{f}_k - \sum_{\mathbf{k}_1}\mathbf{k}_1\times\mathbf{k}_2\cdot\boldsymbol{\epsilon}_\parallel\tilde{\phi}_{k_1}\tilde{f}_{k_2}, \tag{4a}$$

$$\tilde{\nabla}_\parallel\tilde{f}_k = is_k k_\parallel\tilde{f}_k + \beta\sum_{\mathbf{k}_1}\mathbf{k}_1\times\mathbf{k}_2\cdot\boldsymbol{\epsilon}_\parallel\tilde{A}_{k_1}\tilde{f}_{k_2}, \tag{4b}$$

where $\mathbf{k}_2 = \mathbf{k} - \mathbf{k}_1$. In these equations the ion gyrolength $\rho_s = c_s/\Omega$ [where $c_s = (T_e/m_i)^{1/2}$ and $\Omega = eB_0/cm_i$] is the unit of length across the magnetic field $B_0$ and $L_p$ is the unit of length along the field; $L_p/c_s$ is the unit of time. Thus, $k_\parallel = L_p/Rq$ and the diamagnetic drift frequency is $\omega_* = k_y$, where $k_y = (n/qr)\rho_s^{-1}$ represents the poloidal wave number; $k_x$ is the radial wave number. $\beta = \frac{1}{2}p_0/(B_0^2/8\pi)$, where $p_0$ is the equilibrium pressure. The fields are normalized to $\rho_s/L_p$ as follows:

$$\tilde{\phi} = \frac{e\tilde{\Phi}/T_e}{\rho_s/L_p}, \quad \tilde{A} = \frac{e\tilde{A}_\parallel}{T_e}\frac{c_s}{c}\frac{1/\beta}{\rho_s/L_p}, \quad \tilde{P} = \frac{\tilde{p}/p_0}{\rho_s/L_p}.$$

The fields satisfy the reality condition $f_k = f_k^*$ with $s_k = k_y/|k_y|$. The transport coefficient describing the $\tilde{\mathbf{E}}\times\mathbf{B}_0$ diffusion of pressure flux $\langle\tilde{v}_{Ex}\tilde{p}\rangle$ is $\langle D_E\rangle = \langle\sum_k\tilde{\phi}_k^* ik_y\tilde{P}_k\rangle$ in units of $\rho_s^2c_s/L_p$. $\langle\ldots\rangle$ represents the time average.

To single out the linear ideal MHD ballooning stability, let us first set the damping terms represented by the $\gamma$ terms equal to zero. There are three branches

with frequencies $\omega = \pm\omega_{\mathrm{MHD},k}$ and $\omega = 0$, where

$$\omega_{\mathrm{MHD},k} = (k_{\parallel}^2/\beta - gk_y^2/k_{\perp}^2)^{1/2}. \tag{5}$$

They correspond respectively to polarizations $\tilde{\phi}_k^{\pm}$ and $\tilde{P}_k^0$, such that

$$\tilde{\phi}_k = \tilde{\phi}_k^+ + \phi_k^-, \tag{6a}$$

$$\tilde{A}_k = \frac{s_k k_{\parallel}}{\beta\omega_{\mathrm{MHD},k}}(\tilde{\phi}_k^+ - \tilde{\phi}_k^-) + \frac{gk_y}{s_k k_{\parallel} k_{\perp}^2}\tilde{P}_k^0, \tag{6b}$$

$$\tilde{P}_k = \frac{k_y}{\omega_{\mathrm{MHD},k}}(\tilde{\phi}_k^+ - \tilde{\phi}_k^-) + \tilde{P}_k^0. \tag{6c}$$

For $\beta \geq \beta_{\mathrm{crit}} = k_{\parallel}^2/g = L_p/Rq^2$, the curvature drive $g$ (which causes an analog of the Rayleigh-Taylor overturning mode) exceeds the resistance to field-line bending ($k_{\parallel}^2/\beta$), and all modes with $k_x = 0$ first become unstable. In particular, modes with long wavelength ($k_y \to 0$) become unstable. In all the examples treated here $k_{\parallel} = 0.1$ and $g = 0.3$, so that $\beta_{\mathrm{crit}} = 3.3\%$.

The damping terms require special discussion. A standard model for resistive MHD would set $\gamma_k^A = \eta k_{\perp}^2$, where $\eta$ is the classical resistivity, and $\gamma_k^{\phi} = \mu k_{\perp}^2$ and $\gamma_k^P = \kappa k_{\perp}^2$, where $\mu$ and $\kappa$ represent the classical cross-field ion viscosity and heat conductivity. When $\eta$ is sufficiently large compared to $\mu \sim \kappa$ as would be physically the case, the system would be unstable to short-wavelength resistive $g$ (or resistive ballooning modes) (see Waltz,[6] for example). They are unstable at any $\beta$ and in contrast to the ideal modes, their driving rates vanish at long wavelengths ($k_y \to 0$). To clarify the issue of subcritical behavior, I have made the unphysical choice of setting $\gamma_k^{\phi} = \gamma_k^A = \gamma_k^P = \gamma_k^d$. This suppresses the short-wave modes and leaves only the semi-ideal modes $\omega = \pm\omega_{\mathrm{MHD},k} - i\gamma_k^d$ and $\omega = -i\gamma_k^d$ which are damped for $\beta \lesssim \beta_{\mathrm{crit}}$. The model for $\gamma_k^d$ was taken to be

$$\gamma_k^d = \begin{cases} \gamma_0(1 - k_{\perp}^2/k_0^2) + \gamma_m & \text{for } k_{\perp} < k_0, \\ \gamma_m & \text{for } k_0 < k_{\perp} < k_{\infty}, \\ \gamma_{\infty} + \gamma_m & \text{for } k_{\perp} > k_{\infty}, \end{cases}$$

with $-k_{\max} < k_x, k_y < k_{\max}$ ($k_{\max} = 2.25$). This consists of a low-$k$ damping ($\gamma_0 = 0.1$ to $0.5$; $k_0 = 0.8$) to represent the damping via coupling to parallel ion motion or loosely speaking the convective losses to the plasma boundary, and a moderate-$k$ damping ($\gamma_m = 0.0$ or $0.05$) and a high-$k$ damping ($\gamma_{\infty} = 2.0$, $k_{\infty} = 1.9$) to represent the classical cross-field dissipation process. Other choices for the moderate- to high-$k$ damping (e.g., $\gamma_k^d \simeq \mu k_{\perp}^2$) do not change the results. Sufficient low-$k$ damping is essential to avoid complete condensation in the longest wavelengths and lack of stationarity.

Before presenting the results of the simulation, it is useful to write some conservation laws of the system. There are laws for energy and square of the pressure:

$$\frac{d}{dt}\sum_k E_k = gD_E - \sum 2\gamma_k^d E_k, \tag{7a}$$

$$\frac{d}{dt}\sum_k \tilde{P}_k^*\tilde{P}_k/2 = D_E - \sum 2\gamma_k^P \tilde{P}_k^*\tilde{P}_k/2, \tag{7b}$$

where $E_k = (k_{\perp}^2\tilde{\phi}_k^*\tilde{\phi}_k + \beta k_{\perp}^2\tilde{A}_k^*\tilde{A}_k)/2$. Similar laws can be written for the magnetic potential $\sum\tilde{A}_k^*\tilde{A}_k$ and cross helicity $\sum\tilde{\phi}_k^*\tilde{A}_k$. From the time average of (7b), it is clear that one cannot speak of stationary-state turbulence and transport without dissipation in the pressure equation, $\gamma_k^P = \gamma_k^d$ ($\langle D_E\rangle = \sum_k \gamma_k^P\langle|\tilde{P}_k|^2\rangle$). Combining Eqs. (7a) and (7b) results in

$$\frac{d}{dt}\sum_k W_k = -\sum_k 2\gamma_k^2 W_k, \tag{7c}$$

where

$$W_k = (k_{\perp}^2\tilde{\phi}_k^*\tilde{\phi}_k + \beta k_{\perp}^2\tilde{A}_k^*\tilde{A}_k - g\tilde{P}_k^*\tilde{P}_k)/2.$$

It is clear that for $g < 0$ and thus $W_k > 0$, a nonlinear stability theorem results and no turbulence can be sustained.

The simulations were performed on a $31\times31$ grid ($\Delta k = 0.15$) with use of an implicit time step for the advancement of the linear terms and a predictor-corrector for the nonlinear terms. There were typically more than several hundred time steps over the fastest wave period ($\sim 10$ time units at $\beta = 2.5\%$). Cumulative errors in total energy conservation [Eqs. (7a) plus (7b)] were below 1% and no significant changes were observed for time steps 2 and 4 times smaller. Time averages were taken over several hundred time units.

The principal result is shown in Fig. 1 for the marginal damping case $\gamma_m = 0$ with $\gamma_0 = 0.5$. As shown, the transport persists well below the linear critical point. No evidence for hysteresis was found, i.e., the stationary states presented may be approached from many initial conditions. Also shown is a case with $g < 0$ having no turbulence in accord with the nonlinear stability theorem of Eq. (7c). The mixing rule $\tilde{P}_{\mathrm{rms}} \sim (1/k_{\perp})_{\mathrm{rms}}$ is roughly satisfied with $(1/k_{\perp})_{\mathrm{rms}} \sim 1$. The spectra are roughly isotropic. As the low-$k$ damping $\gamma_0$ is diminished, more condensation in the longest wavelengths is allowed [$(1/k_{\perp})_{\mathrm{rms}}$ increases] and the transport increases dramatically beyond $\beta > \frac{1}{2}\beta_{\mathrm{crit}}$. Figure 2 shows that the subcritical turbulence persists in the damped case $\gamma_m = 0.05$ at least for $\beta > \frac{1}{2}\beta_{\mathrm{crit}}$. These cases require some sufficiently strong perturbations to initiate them. The tendency for the onset of long-wavelength condensation and catastrophic transport at $\beta > \frac{1}{2}\beta_{\mathrm{crit}}$ was a general feature of similar two- and three-fluid models with linear dissipative instabilities treated in earlier work.[6] In reality the dissipative instabilities could easily pro-

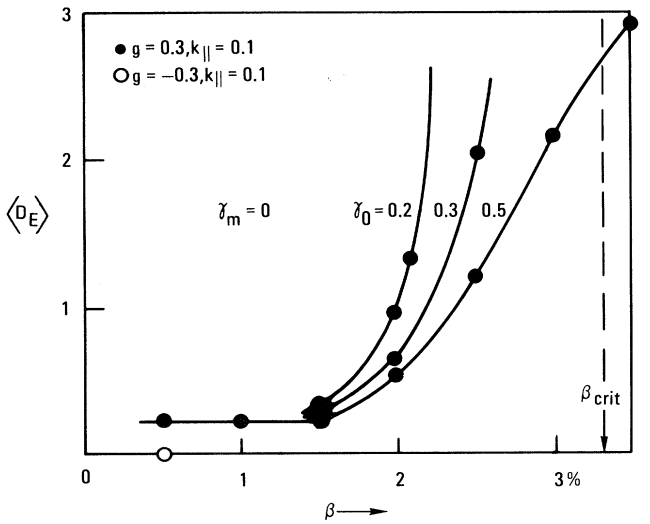


FIG. 1. Transport coefficients vs $\beta$ for the marginal damping case ($\gamma_m = 0.0$).

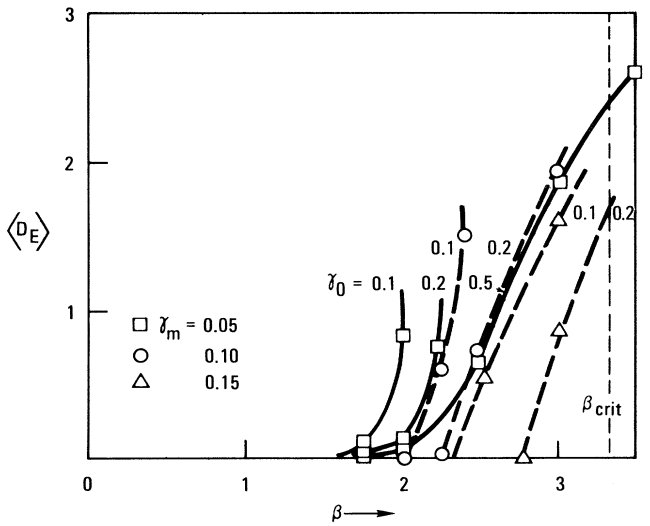


FIG. 2. Transport coefficients vs $\beta$ for the damped case ($\gamma_m > 0.0$).

vide the excitation to initiate the ideal subcritical turbulence. As the damping is increased to $\gamma_m = 0.10$ and 0.15 the subcritical onset is less pronounced.

While long-wavelength condensation is clearly a phenomenon of systems with large numbers of waves, the basic mechanism for nonlinear instability can operate even in a three-wave system. In particular, Eqs. (1) through (4) simulated with a triplet representation $\mathbf{k} = \pm\{(1,0);(0,1);(\sqrt{2},\sqrt{2})\}$ of equally damped waves, $\gamma_k^d = \gamma_m = 0.05$ to 0.10, exhibit subcritical chaotic motion (strange attractor) provided that sufficient initial excitation is given. An order-of-magnitude smaller time steps and longer simulation times may now be used. A larger damping rate ($\gamma_m = 0.2$) destroys the effect, while an intermediate rate ($\gamma_m = 0.15$) allows nearly stationary chaotic motion which can "sputter off." After a linear damping period, the system evolves to the $W \cong 0$ state [see Eq. (7c)] since all $\gamma_k^d$ are equal In addition, $\langle D\rangle = 2\gamma_m\langle E\rangle/g = \gamma_m \tilde{P}^2_{\rm rms}$ from Eqs. (7a) and (7b). $\langle D\rangle \simeq 2$ is weakly dependent on $\beta$ up to $\beta \lesssim \beta_{\rm crit}$ where it increases dramatically. "Turning off" the nonlinear terms in midcourse allows the system to decay at the linear rate.

Some aspects of the subcritical turbulence seen here may be understood by application of the ideas which have served so well in explaining plane-parallel pipe flow.[2,3] In that case one looks for secondary equilibria (or near equilibria) which can be shown to exist down to the lowest Reynolds numbers at which the turbulence is observed in experiments and simulations. The secondary equilibria are two-dimensional coherent motions superposed on the straight streamline motion of the primary equilibria. They are then shown to be violently unstable to three-dimensional perturbations.

In general, for the MHD model it is difficult to find the secondary equilibria. This requires the solution of the nonlinear algebraic equations formed by setting $\tilde{d}/dt = 0$ (or $i\mathbf{c}\cdot\mathbf{k}$) in Eqs. (1) to (4). Even in the triplet case this is a system with eighteen degrees of freedom (less two phase angles) and no solution has yet been found. However, in the many-wave case with marginal damping $\gamma_m = 0$, each linear $\omega = 0$ wave with $k_0 < k_\perp < k_\infty$ is a separate equilibrium. (Note that a single linear wave can be a solution to the nonlinear equations.) It is straightforward to test for linear instability about such a secondary equilibrium acting as a pump wave with wave number $\underline{k}$ and strength $\tilde{P}^0_{\underline{k}}$. From Eq. (6) the pump has

$$\tilde{\phi}_{\underline{k}} = 0, \quad \tilde{A}_{\underline{k}} = \underline{k}_y g \tilde{P}^0_{\underline{k}} / s_{\underline{k}} k_{\|} \underline{k}_\perp^2,$$

and $\tilde{P}_{\underline{k}} = \tilde{P}^0_{\underline{k}}$. A coupled linear eigenvalue problem results:

$$-i\omega k_\perp^2 \tilde{\tilde{\phi}}_k = ig\omega_* \tilde{\tilde{P}}_k - ik_{\|} s_k k_\perp^2 \tilde{\tilde{A}}_k - \gamma_k^d k_\perp^2 \tilde{\tilde{\phi}}_k$$
$$-\beta \underline{\mathbf{k}}\times\mathbf{k}\cdot\boldsymbol{\epsilon}_{\|}[(k-\underline{k})^2 - \underline{k}^2]\tilde{\tilde{A}}_{k-\underline{k}}\tilde{A}_{\underline{k}} + \beta\underline{\mathbf{k}}\times\mathbf{k}\cdot\boldsymbol{\epsilon}_{\|}[(k+\underline{k})^2 - \underline{k}^2]\tilde{\tilde{A}}_{k+\underline{k}}\tilde{A}^*_{\underline{k}}, \tag{8a}$$

$$-i\omega\tilde{\tilde{A}}_k = -(ik_{\|}/\beta)s_k\tilde{\tilde{\phi}}_k - \gamma_k^d\tilde{\tilde{A}}_{\underline{k}} - \underline{\mathbf{k}}\times\mathbf{k}\cdot\boldsymbol{\epsilon}_{\|}(\tilde{\tilde{\phi}}_{k-\underline{k}}\tilde{A}_{\underline{k}} - \tilde{\tilde{\phi}}_{k+\underline{k}}\tilde{A}^*_{\underline{k}}), \tag{8b}$$

$$-i\omega\tilde{\tilde{P}}_k = -i\omega_*\tilde{\tilde{\phi}}_k - \gamma_k^d\tilde{\tilde{P}}_k - \underline{\mathbf{k}}\times\mathbf{k}\cdot\boldsymbol{\epsilon}_{\|}(\tilde{\tilde{\phi}}_{k-\underline{k}}\tilde{P}_{\underline{k}} - \tilde{\tilde{\phi}}_{k+\underline{k}}\tilde{P}^*_{\underline{k}}). \tag{8c}$$

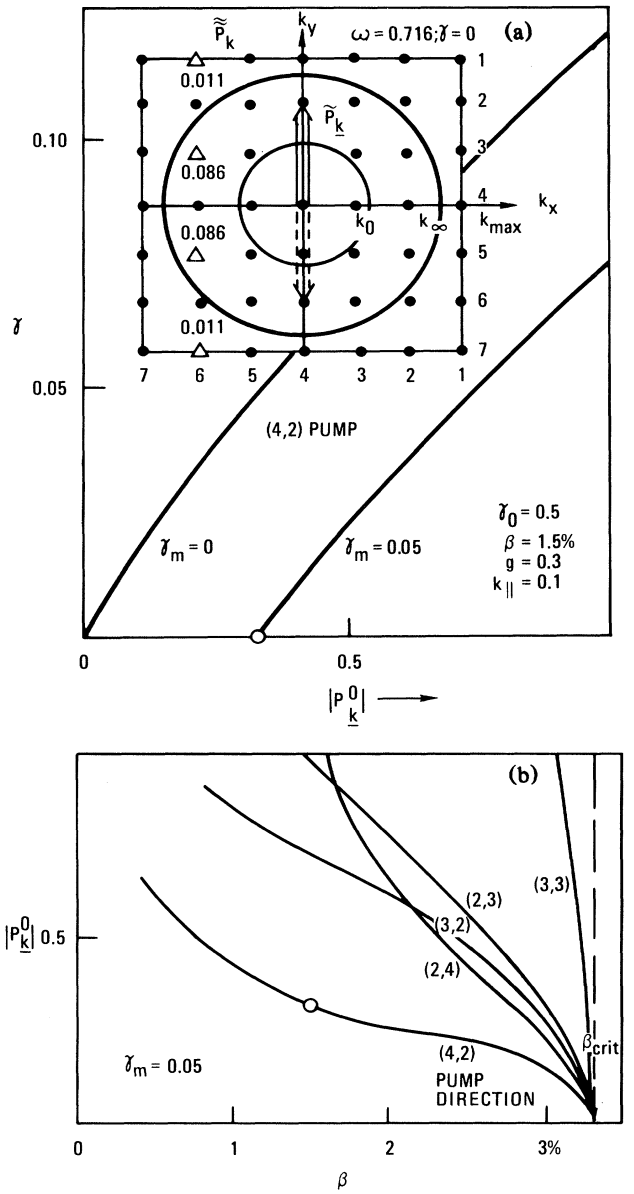


FIG. 3. (a) Secondary-instability growth rate vs pump-wave amplitude strength. The lowest pump direction ($\tilde{P}_{\underline{k}}$) and mode wave function ($\tilde{\tilde{P}}_{\underline{k}}$) are shown in the inset $7\times7$ grid as the arrow and the triangles with relative weights, respectively. Circles indicate boundaries of low-$k$ ($k_0$) and high-$k$ ($k_\infty$) damping. (b) Pump-wave strength vs $\beta$ for damped case.

(Without loss of generality we can choose the phase to be $\tilde{P}^0_{\underline{k}} = \tilde{P}^{0*}_{-\underline{k}} = i|\tilde{P}^0_k|$.) If the number of modes is reduced from $31\times31$ to $7\times7$, matrix inversion for the solution of Eq. (8) is easily managed. A pump wave in the $k_y$ direction is most effective. As shown in Fig. 3(a), an infinitesimal pump strength is sufficient to produce instability (at all but the smallest $\beta$). The lowest eigenfunction and pump are shown in the inset. This appears to be sufficient to explain the existence of turbulence at all $\beta$ in the marginal damping case $\gamma_m = 0$ of Fig. 1. As damping is added in the region $k_0 < k_\perp < k_\infty$ ($\gamma_m = 0.05$), the pump wave must acquire finite amplitude to drive the system unstable. Figure 3(b) shows that pump waves in other directions require larger strengths. In the damped case, however, the single $\omega = 0$ linear wave pump is itself damped and does not represent a secondary equilibrium. A nonlinear state is required.

In summary, a simple two-dimensional model for MHD ballooning modes has shown subcritical turbulence. In partial analogy with the theory of plane-parallel pipe flow, the result appears to be consistent with instability about a zero-frequency wave acting as a secondary equilibrium at least in the limiting case of marginal damping. The propensity for sudden onset of long-wavelength condensation and catastrophic transport at $\beta \gtrsim \frac{1}{2}\beta_{\rm crit}$ is the most important feature of the subcritical turbulence. Unlike the pipe-flow case, the critical threshold remains unexplained in general. It is my hope that the present work with a very simplified two-dimensional homogeneous model will motivate the search for subcritical turbulence with more physically realistic three-dimensional boundary-value MHD simulation codes.

This work was initiated during an exchange visit at the United Kingdom Atomic Energy Authority Culham Laboratory, Abingdon, England. I want to thank the members of the Culham theory group for their hospitality. I am indebted to a number of colleages for discussions of subcritical turbulence, and I particularly want to thank Dr. John M. Greene for numerous discussions and encouragement. This work was supported by the U. S. Department of Energy under Contract No. De-AT03-84ER53158.

[1]D. Montgomery, Phys. Scr. **T2**, 506 (1982).

[2]S. A. Orszag and L. D. Kells, J. Fluid Mech. **96**, 159 (1980).

[3]A. A. Orszag and A. T. Patera, in *Transition and Turbulence,* edited by R. E. Meyer (Academic, New York, 1981), p. 127; J. T. Stuart, *ibid.*, p. 77.

[4]R. H. Berman, D. Tetreault, T. H. Dupree, and T. Boutros-Ghali, Phys. Rev. Lett. **48**, 1249 (1982).

[5]M. Walter and D. Biskamp, in Proceedings of Sherwood Theory Conference, Incline Village, Nevada, April 1984 (unpublished), paper 2R5.

[6]R. E. Waltz, Phys. Fluids **28**, 577 (1985).